ISSN 1063-7737, Astronomy Letters, 2009, Vol. 35, No. 5, pp. 294–304. © Pleiades Publishing, Inc., 2009.
Original Russian Text © I.G. Prokopenko, M.R. Gilfanov, 2009, published in Pis'ma v Astronomicheskiĭ Zhurnal, 2009, Vol. 35, No. 5, pp. 330–341.

# Normal Galaxies in the All-Sky Survey by the eROSITA X-ray Telescope of the Spectrum-X-Gamma Observatory

**I. G. Prokopenko[1,2*] and M. R. Gilfanov[1,2]**

[1] *Space Research Institute, Russian Academy of Sciences, Profsoyuznaya ul. 84/32, Moscow, 117997 Russia*
[2] *Max-Planck-Institut für Astrophysik, Karl-Schwarzschild-Str. 1, Postfach 1317, D-85741 Garching, Germany*

Received August 18, 2008

**Abstract**—We analyze the statistical properties of normal galaxies to be detected in the all-sky survey by the eROSITA X-ray telescope of the Spectrum-X-Gamma observatory. With the current configuration and parameters of the eROSITA telescope, the sensitivity of a 4-year-long all-sky survey will be $\approx 10^{-14}$ erg s$^{-1}$ in the 0.5–2 keV band. This will allow $\sim(1.5–2)\times 10^4$ normal galaxies with approximately the same contribution of star-forming and elliptical galaxies to be detected. All galaxies of the X-ray survey are expected to enter into the existing far-infrared (IRAS) or near-infrared (2MASS) catalogs; the sample of star-forming galaxies will be approximately equivalent in sensitivity to the sample of star-forming galaxies in the IRAS catalog of infrared sources. Thus, a large homogeneous sample of normal galaxies with measured X-ray, near-infrared, and far-infrared fluxes will be formed. About 90% of the galaxies in the survey are located within ∼200–400 Mpc. A typical (most probable) galaxy will have a luminosity $\log L_X \sim 40.5–41.0$, will be located at a distance of ∼70–90 Mpc, and will be either a star-forming galaxy with a star formation rate of $\sim 20 M_\odot$ yr$^{-1}$ whose X-ray emission is produced by ultraluminous X-ray sources (ULXs) or an elliptical galaxy with a mass $\log M_* \sim 11.3$ emitting through to a hot interstellar gas. The galaxies within 35 Mpc will collectively contain $\sim 10^2$ ULXs with luminosities $\log L_X > 40$, ∼80% of which will be the only luminous source in the galaxy. Thus, although the angular resolution of the eROSITA telescope is too low for the luminosity function of compact sources in galaxies to be studied in detail, the survey data will allow one to investigate its bright end and, possibly, to impose constraints on the maximum luminosity of ULXs.

PACS numbers : 98.70.Qy
**DOI:** 10.1134/S1063773709050028

Key words: *normal galaxies, ultraluminous X-ray sources, X-ray surveys, Spectrum-X-Gamma observatory.*

## INTRODUCTION

The eROSITA X-ray telescope is one of the main instruments onboard the Spectrum-X-Gamma observatory to be launched into orbit in 2011. One of the main elements of the scientific program of the observatory will be an all-sky survey whose expected duration will be 4 years. After completion of the survey, a transition to the observations of individual extragalactic and galactic sources in the regime of triaxial stabilization for 3–6 years is planned. The main objectives of the future observatory are the studies of the nature of dark energy and dark matter, in particular, based on the investigation of a large number of galaxy clusters to be detected during the all-sky survey. In addition, a considerable number of active galactic nuclei and normal galaxies will be detected in four years of the all-sky survey. Thus, eROSITA can become an important instrument for studying galaxies in X-rays. In this paper, we analyze various statistical properties of a sample of normal galaxies to be detected during the all-sky survey by the eROSITA X-ray telescope.

Here, we use the following cosmological parameters: $H_0 = 100h$ km s$^{-1}$ Mpc$^{-1}$, $h = 0.7$ ($\Omega_M$, $\Omega_\Lambda$, $\Omega_K$) = (0.3, 0.7, 0), where $H_0$ is the present value of the Hubble constant, $\Omega_M$ and $\Omega_\Lambda$ are, respectively, the mean densities of the matter and dark energy in the Universe in units of the critical density. These cosmological parameters have been universally accepted in the studies of the luminosity functions and number counts of extragalactic sources. They are close to the values obtained from the data of the 3-year-long operation of the WMAP satellite (Spergel et al. 2007).

*E-mail: prokopenko@iki.rssi.ru

## SENSITIVITY OF THE ALL-SKY SURVEY BY THE eROSITA X-RAY TELESCOPE

The eROSITA X-ray telescope consists of seven Wolter-I-type (paraboloid + hyperboloid) mirror systems with a CCD detector mounted at the focus of each system. The field of view for each telescope is 1.03° in diameter, the angular resolution (half-power diameter) averaged over the field of view is 29″ at 1.5 keV, the energy band is 0.5–10 keV, and the energy resolution (full width at half maximum) is 130 eV at 6 keV. The total effective area of the seven mirror systems averaged over the field of view at maximum, at ∼1.5 keV, reaches ≈1450 cm$^2$ and decreases to ≈80 cm$^2$ at 6 keV (http://www.mpe.mpg.de/erosita, http://hea.iki.rssi.ru/SXG/PROJECT/SXG-eng.htm). To calculate the sensitivity, we will use a preliminary eROSITA response matrix averaged over the field of view (erosita_iii_7telfov_ff.rsp; P. Predehl 2008, private communication).

The sensitivity of the survey is determined by the average observing time for a given (arbitrary) direction and also depends on the source spectrum and background characteristics. Disregarding the specific configuration of the sky scans during the survey, which has not yet been completely determined, we will estimate the average observing time as the product of the total survey time (4 years), given the efficiency of using the observing time (∼90%), by the ratio of the eROSITA field of view to the (all-sky) survey area: $t_{\rm obs} \approx 2300 \times \left(t_{\rm survey}/(4\ {\rm yr})\right) \times (f_{\rm eff}/0.9)$ s.

The following components make a major contribution to the background of the eROSITA telescopes: the cosmic X-ray background (CXB), high-energy cosmic rays, and solar protons with energies of the order of several hundred keV, which can be focused by the mirrors of the X-ray telescopes. The role of the last two factors depends significantly on the orbit, which has not yet been completely determined for Spectrum-X-Gamma. For a low-apogee orbit, their contribution may be neglected. For a high-apogee orbit, the effect of low-energy protons can be reduced significantly using magnetic deflectors, whose installation on eROSITA is being considered.

Let us estimate the number of counts related to the CXB. Its spectrum in the 0.5–8 keV band can be well described by a two-component model (Hickox and Markevitch 2006) that consists of (i) the spectrum of an optically thin plasma (the APEC model in the XSPEC package; Smith et al. 2001) with a temperature $kT \sim 0.15$ keV related to the diffuse Galactic background and (ii) a power-law spectrum with a photon index $\Gamma = 1.4$ and absorption $N_{\rm H} \approx 1.5 \times 10^{20}$ cm$^{-2}$ that includes the contribution from extragalactic sources. To estimate the sensitivity of the survey, we should exclude the part of the CXB that is produced by bright extragalactic sources and that will be spatially resolved by eROSITA into individual objects. It follows from the observed number counts of extragalactic sources in the 0.5–2-keV band (Moretti et al. 2003) that the contribution from bright sources with fluxes $F_{0.5-2\,{\rm keV}} > 10^{-14}$ erg s$^{-1}$ cm$^{-2}$ to the power-law component is ∼50%. Therefore, for a simple estimate, we reduced the normalization of the power-law component in the CXB model spectrum by a factor of 2. The exact fraction of resolved extragalactic sources does not affect strongly the final result, since the contribution from the soft component related to the Galactic emission to the CXB spectrum in the 0.5–2-keV band is ∼35%, while the role of the CXB in a harder energy band is marginal. Convolving this spectrum with the response matrix of the eROSITA detectors yields the total count rate for the seven telescopes, ≈5 counts per second per field of view. Inside the region of half-power diameter (HPD) of the point spread function (PSF) (a circle 29″ in diameter, within which half of the photons from the source are contained), we obtain ≈0.7 photons from the CXB in the 0.5–2 keV band over an exposure time of 2300 s corresponding to 4 years of the survey (seven telescopes). Assuming that the counts from the background obey a Poisson distribution, the probability that more than 9 photons from the background will be detected by chance in the region of response to a point source is $\approx 5.9 \times 10^{-8}$, which corresponds to one false source in $\sim 10^3$ fields of view (∼40 false source in the entire sky).[1] Since half of the photons from the source are contained within the circle 29″ in diameter, this detection limit corresponds to 18 photons from the source. This detection limit will also allow the fluxes from sources to be determined with an accuracy better than ∼30%, which is of great importance, in particular, in constructing the curves of source numbers counts and luminosity functions. A similar calculation for the 2–8 keV band gives ≈0.08 photons from the CXB in 4 years of the all-sky survey. The probability that more than 5 photons from the background will be detected by chance in the region of response to a point source is $\approx 2.6 \times 10^{-8}$, which corresponds to one false source in $\sim 2.3 \times 10^3$ fields of view. In this case, the detection limit corresponds to 10 photons from the source in the 2–8 keV band.

To roughly estimate the cosmic-ray background level, we used data for the instrumental background of the XMM-Newton telescope. Assuming that the number of counts produced by cosmic rays was proportional to the total geometric area of the detectors,

[1] Lowering the detection threshold causes a rapid increase in the number of false sources. For example, a detection threshold of 7 photons corresponds to $\sim 6 \times 10^3$ false sources in the entire sky.

we recalculated the observed data for the XMM-Newton instrumental background to the area of the eROSITA detectors ($28.8 \times 28.8\,\mathrm{mm}^2 \times 7$). We found the count rate of the cosmic-ray background for eROSITA to be $\approx$3.2 counts $\mathrm{s}^{-1}$, which corresponds to $\approx$0.4 counts inside the region of half-power diameter of the PSF in 4 years of the all-sky survey. This value is a factor of $\sim$2 lower than the contribution from the CXB in the soft energy band but it can become crucial in the 2–8 keV band and can cause a rise in the detection threshold in the hard energy band by a factor of $\gtrsim$1.5. In the subsequent calculations, we will use the sensitivities obtained above by taking into account only the CXB contribution, since the role of cosmic rays is determined by the orbit of the Spectrum-X-Gamma observatory, which has not yet been completely determined. This choice of the background corresponds to a low-apogee orbit.

Assuming a power-law spectrum with a photon index $\Gamma = 1.8$ and absorption $N_\mathrm{H} = 3 \times 10^{20}$ $\mathrm{cm}^{-2}$ typical of normal galaxies, let us convert the derived detection thresholds into flux units:

$$S_0(0.5\text{–}2\ \mathrm{keV}) = 1.0 \times 10^{-14}\ \mathrm{erg\ s^{-1}\ cm^{-2}},$$

$$S_0(2\text{–}8\ \mathrm{keV}) = 1.0 \times 10^{-13}\ \mathrm{erg\ s^{-1}\ cm^{-2}}.$$

The sensitivity in the 0.5–2 keV band for the spectrum of an optically thin plasma with a temperature $kT = 0.7$ keV ($N_\mathrm{H} = 3 \times 10^{20}$ $\mathrm{cm}^{-2}$) typical of elliptical galaxies emitting through a hot interstellar gas differs from the above one by $\sim$10%. Note that these sensitivity limits are fairly conservative. In several situations, for example, when searching for sources in a bounded sky field or when their positions are known, fainter sources can be detected. In addition, depending on the configuration of the scans, the observing time for individual sky fields can exceed significantly the average value; accordingly, the sensitivity of the survey in such sky regions will be higher.

The sensitivities given above correspond to the detection threshold of point sources. The angular resolution of the eROSITA telescope, 29″ HPD (half-power diameter), corresponds to a linear size of $\approx$10 kpc at a distance of 70 Mpc. Therefore, the nearest galaxies, $D \lesssim 50$–70 Mpc, will be observed as extended sources. Assuming that the characteristic size of an X-ray-bright region is 15 kpc, let us estimate the sensitivity for a galaxy located at a distance of 35 Mpc. The number of counts from the CXB within the circle 90″ in diameter will be $\approx$6.3 in 2300 s; a detection threshold of 23 counts will correspond to approximately the same number of false sources in the survey as that for the above sensitivity thresholds. Thus, the sensitivity will drop due to the spatial extent of nearby galaxies by a factor of $\sim$2. The exact value depends on the angular distribution of the emission. Thus, for example, for elliptical galaxies, the drop in sensitivity will be smaller due to the concentration of emission toward the galactic center. As will be shown below (see, e.g., Fig. 3), the fraction of the galaxies located within $\sim$50–70 Mpc does not exceed $\sim$10–15%. Therefore, a reduction in the sensitivity for nearby objects will not affect significantly the statistical properties and average characteristics of the galaxies in the survey that are the subject of this paper. Note also that the nearest galaxies located at distances $\lesssim$20 Mpc will be spatially resolved into bright sources (see the section devoted to ultraluminous X-ray sources).

## THE $\log N - \log S$ FOR STAR-FORMING GALAXIES

To estimate the number of galaxies of various types to be detected in the survey, their $\log N - \log S$ must be known. The major observational programs of the Chandra and XMM-Newton observatories are devoted to the investigation of these curves for X-ray sources. However, the $\log N - \log S$ for normal galaxies have been studied comparatively poorly mainly because of their relatively small number in the existing surveys and the difficulty of their separation from the much more numerous active galactic nuclei and quasars. In the soft 0.5–2.0 keV band, these curves are known from the Chandra and XMM-Newton surveys but their accuracy is limited for the reasons given above. At present, there are virtually no number counts of normal galaxies in the hard energy band. Therefore, our predictions are based on the theoretical $\log N - \log S$ obtained by integrating the luminosity functions of galaxies and we use the available number counts of normal galaxies in the soft energy band to check our calculations. This approach also allows the distributions of observable galaxies in various parameters, such as the distance, luminosity, mass, and star formation rate, to be found without any difficulty.

The theoretical curve of galaxy number counts can be obtained by integrating the luminosity function over the entire range of redshifts $z$:

$$N(>S) = \int_0^\infty dz \frac{dV}{dz} \int_{L_\mathrm{min}(S,z)}^{L_\mathrm{max}} \phi(\log L, z)\, d\log L, \quad (1)$$

where $\phi(\log L, z)$ [$\log L^{-1}$, $\mathrm{Mpc}^{-3}$] is the galaxy luminosity function, $S$ [$\mathrm{erg\ s^{-1}\ cm^{-2}}$] is the flux, $L$ [$\mathrm{erg\ s^{-1}}$] is the luminosity, $D_L(z)$ is the luminosity distance, and $L_\mathrm{min}(S,z) = 4\pi S D_L^2(z)$. When calculating $L_\mathrm{min}(S,z)$, we should apply the $K$ correction. Note that this effect is negligible for a power-law spectrum with a photon index of 1.8. Currently, the flux-limited catalogs of star-forming galaxies in

the X-ray band from which the luminosity function is determined are relatively small (contain ∼30–50 galaxies; see, e.g., Georgakakis et al. 2006a). The luminosity functions of these galaxies are known statistically much better at other wavelengths, in particular, in the radio band at 1.4 GHz (∼500 galaxies; Machalski and Godlowski 2000). Following the standard method, we used the correlation between the X-ray and radio luminosities (Ranalli et al. 2003, 2005) to indirectly estimate the X-ray luminosity function: $\log L_{1.4\,\mathrm{GHz}} = \log L_{0.5-2\,\mathrm{keV}} - 11.08$, where $L_{0.5-2\,\mathrm{keV}}$ is expressed in erg s$^{-1}$ and $L_{1.4\,\mathrm{GHz}}$ has the dimensions of erg s$^{-1}$ Hz$^{-1}$. Thus, we can pass from the known radio (1.4 GHz) luminosity function of star-forming galaxies to the X-ray (0.5–2 keV) luminosity function. The shape of the radio luminosity function can be well fitted by the expression (Machalski and Godlowski 2000)

$$\phi(L) = \phi^* \left(\frac{L}{L^*}\right)^{1-\alpha} \times \exp\left[-\frac{1}{2\sigma^2}\log^2\left(1+\frac{L}{L^*}\right)\right], \quad (2)$$

where $\phi^* = (7.9^{+3.8}_{-2.6}) \times 10^{-3} h^3$ [Mpc$^{-3}/d\log L$], $\log L^* = (28.13 \pm 0.37) - 2\log h$ [erg s$^{-1}$ Hz$^{-1}$], $\alpha = 1.22 \pm 0.27, \sigma = 0.61 \pm 0.05$.

To construct the curve of star-forming galaxy number counts, we should make another assumption about the evolution of the X-ray luminosity function.[2] The Chandra and XXM-Newton observational data for this type of galaxies suggest that the evolution of the luminosity function can be described by the luminosity evolution: $L^*(z) \sim (1+z)^p$, where $p \sim 2.3$–$2.7$ (Georgakakis et al. 2006a; Ptak et al. 2007; Georgantopoulos and Tzanavaris 2008). On the whole, this result is consistent with the assumption that star formation takes place mostly in normal galaxies with $L \sim L^*$. Since the X-ray luminosity of star-forming galaxies is proportional to the star formation rate, the evolution of the X-ray luminosity function may be assumed to closely follow the cosmological star formation history $SFR(z)$, i.e., $L^*(z) \sim SFR(z)$. These two variants of evolution do not contradict each other up to a redshift of ∼2. We will perform our calculation for $L^*(z) \sim (1+z)^{2.5}$ at $z < 2$ and $L^*(z > 2) = \mathrm{const}$. Note that the galaxies in the survey are located within ∼300–500 Mpc (see the section devoted to the distance distribution of galaxies). At such distances, the application of the evolution model described above may not be quite justifiable, since it is based on the deeper Chandra and XMM-Newton surveys. However, comparison with the calculations without any evolution shows that the results differ by no more than ∼10% in the range of fluxes corresponding to the sensitivity of the eROSITA survey. The curve of star-forming galaxy number counts in the 0.5–2 keV band obtained from the observed radio (1.4 GHz) luminosity function is shown in Fig. 1. This figure also presents the curve of galaxy number counts constructed from the observed X-ray luminosity function of late-type galaxies in the 0.5–2 keV band (Georgakakis et al. 2006a) with the same variant of evolution:

$$\phi(L) = \phi^* \left(\frac{L}{L^*}\right)^{1+\alpha} \exp\left(-\frac{L}{L^*}\right), \quad (3)$$

where $\phi^* = (6.0^{+7.3}_{-3.8}) \times 10^{-4}$ [Mpc$^{-3}/d\log L$], $\alpha = -1.61^{+0.20}_{-0.17}$, $\log L_* = 40.65^{+0.17}_{-0.14}$ [erg s$^{-1}$]. For comparison, Fig. 1 shows the observed $\log N - \log S$ (Georgakakis et al. 2006b). The points correspond to the Chandra observations in the range of faint fluxes, $f_X(0.5-2\,\mathrm{keV}) \approx 10^{-17}$–$10^{-15}$ erg s$^{-1}$ cm$^{-2}$,

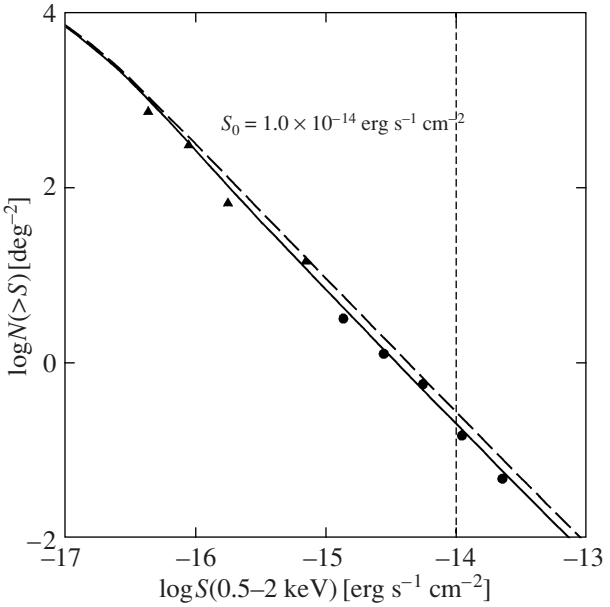


**Fig. 1.** Star-forming galaxy number counts in the 0.5–2 keV band. The solid and dashed lines indicate, respectively, the curves obtained by integrating the observed X-ray luminosity function of late-type galaxies and by integrating the radio luminosity function. The symbols represent the observed late-type galaxy number counts from Chandra (triangles) and XMM-Newton (circles) data (Georgakakis et al. 2006b). The vertical line indicates the sensitivity limit of the 4-year-long all-sky survey.

[2] Although the evolution does not play a major role in determining the number of galaxies in the eROSITA survey, it is important to take into account the evolution of the luminosity function to compare the galaxy number counts obtained by integrating the luminosity function with the Chandra and XXM-Newton observational data in the range of faint fluxes, $f_X(0.5-2\,\mathrm{keV}) \lesssim 10^{-16}$ erg s$^{-1}$ cm$^{-2}$.

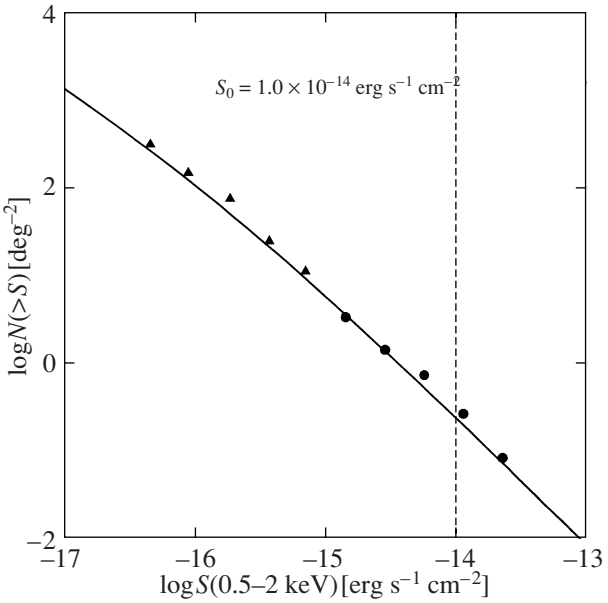


**Fig. 2.** Elliptical galaxy number counts in the 0.5–2 keV band. The solid line indicates the curve obtained by integrating the observed X-ray luminosity function of early-type galaxies. The symbols represent the observed number counts from Chandra (triangles) and XMM-Newton (circles) data (Georgakakis et al. 2006b). The vertical line indicates the sensitivity limit of the 4-year-long all-sky survey.

and to the XMM-Newton observations in the range $f_X(0.5–2\,\mathrm{keV}) \approx 10^{-15}–10^{-13}$ erg s$^{-1}$ cm$^{-2}$. The derived curves of galaxy number counts agree well with the observed points. Note that this fact is trivial for the $\log N - \log S$ calculated using the X-ray luminosity function, since the latter was constructed from the same observational data as those shown in the figure. At the same time, the radio luminosity function and, accordingly, the $\log N - \log S$ calculated using it is completely independent of the X-ray data.

Using the derived $\log N - \log S$, let us estimate the number of star-forming galaxies to be detected in the all-sky survey by the eROSITA telescope. In this case, the Galactic disk region $|b| < 10°$, which is characterized by a higher and inhomogeneous absorption and is affected by the emission from the Galactic ridge, will be excluded from consideration. The derived curves of counts show that ~7200–10 000 late-type galaxies will be detected during the all-sky survey by the eROSITA telescope in the 0.5–2.0 keV band.

To estimate the number of star-forming galaxies in the 2–8 keV band, we also used two approaches based on the observed X-ray and radio luminosity functions. The X-ray luminosity function determined for the 0.5–2 keV band was transformed to that in the 2–8 keV band by assuming a power-law spectrum with a photon index of 1.8 and absorption $N_H = 3 \times 10^{20}$ cm$^{-2}$. To transform the observed radio (1.4 GHz) luminosity function, we used the correlation between the X-ray and radio luminosities, $\log L_{1.4\,\mathrm{GHz}} = \log L_{2–10\,\mathrm{keV}} – 11.13$ (Ranalli et al. 2003). Our calculations using Eq. (1) for the flux corresponding to the sensitivity of the eROSITA survey, $S_0(2–8\,\mathrm{keV}) = 1.0 \times 10^{-13}$ erg s$^{-1}$ cm$^{-2}$, give an estimate of ~300–400 late-type galaxies.

## THE $\log N - \log S$ FOR ELLIPTICAL GALAXIES

To determine the theoretical curve of elliptical galaxy number counts, we used the observed luminosity function of early-type galaxies in the 0.5–2 keV band (Georgakakis et al. 2006a) constructed from a catalog of 34 galaxies. Attempts to obtain the X-ray luminosity function of elliptical galaxies indirectly, for example, from the $K$-band luminosity function and using the correlations between the X-ray and optical luminosities for a hot interstellar gas (O'Sullivan et al. 2001) and low-mass X-ray binaries (LMXBs) (Gilfanov 2004), lead to strong disagreement (by a factor of ~3–5) with the observed luminosity function in the 0.5–2 keV band. This fact was also pointed out, for example, by Georgantopoulos and Tzanavaris (2008): the luminosity function of early-type galaxies obtained from the optical luminosity function and from the correlation between the X-ray and optical luminosities overestimates the observed 0.5–2 keV luminosity function in all luminosity ranges. This may result from the selection effect when the relation between the hot-gas X-ray luminosity and the galaxy optical luminosity is determined. The relation derived from the elliptical galaxies selected on the basis of their X-ray properties may not be applicable to all galaxies. Since an investigation of this effect is beyond the scope of this paper, we restricted ourselves to constructing the elliptical galaxy number counts based on their X-ray luminosity function.

The observed evolution of the X-ray luminosity function for early-type galaxies is appreciably weaker than that for late-type ones (Georgakakis et al. 2006a; Ptak et al. 2007; Georgantopoulos and Tzanavaris 2008). Therefore, for our calculations, we will consider the variant without evolution. This assumption can affect the shape of the $\log N - \log S$ curve in the range of faint fluxes, $f_X(0.5–2\,\mathrm{keV}) < 10^{-16}$ erg s$^{-1}$ cm$^{-2}$, while its effect is weak in the eROSITA sensitivity range. We used the observed luminosity function of early-type galaxies in the 0.5–2 keV band (Georgakakis et al. 2006a)

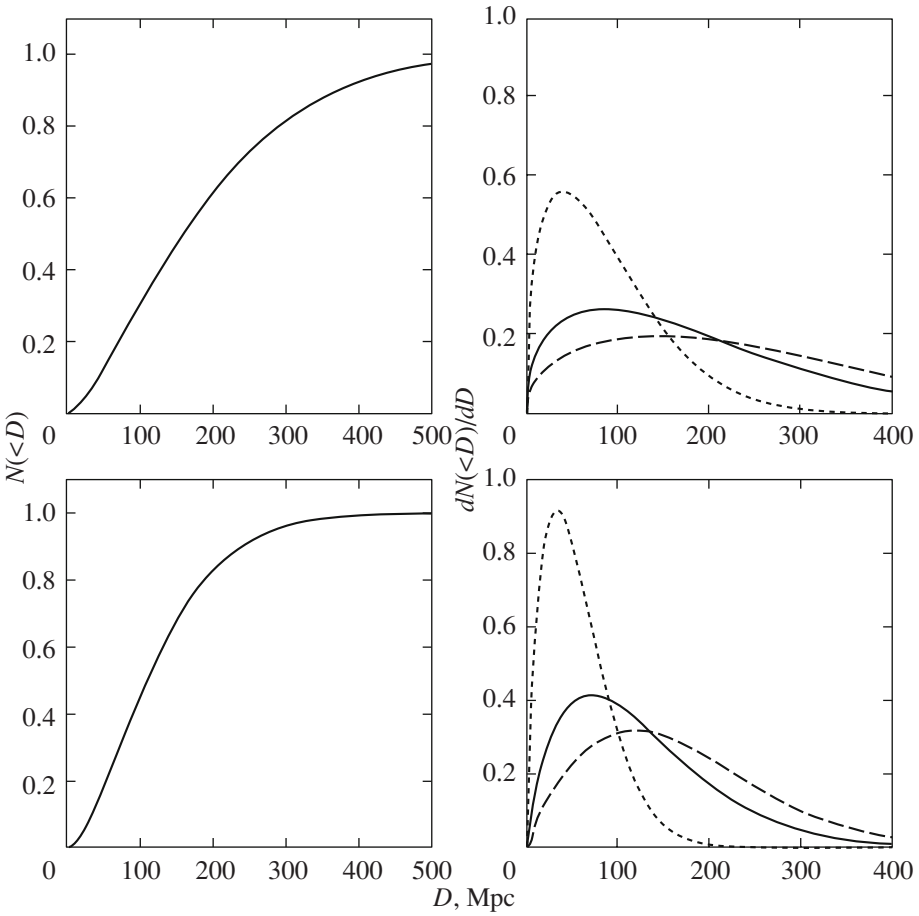


**Fig. 3.** Expected cumulative (left) and differential (right) distance distributions of star-forming (bottom) and elliptical (top) galaxies in the survey in the 0.5–2 keV band. The right panels show the distributions of the complete sample of galaxies (solid line), 10% of the brightest (dotted line) and 10% of the faintest (dashed line) galaxies. The normalization of all differential distributions on the right panels is the same.

with a fit in the form (3) and the following parameters: $\phi^* = (0.9^{+1.1}_{-0.4}) \times 10^{-4}$ [Mpc$^{-3}/d\log L$], $\alpha = -1.79^{+0.13}_{-0.14}$, $\log L_* = 41.25^{+0.25}_{-0.18}$ [erg s$^{-1}$]. The theoretical curve of counts calculated using Eq. (1) is shown in Fig. 2. Also shown in Fig. 2 is the observed $\log N - \log S$ curve for early-type galaxies (Georgakakis et al. 2006b). The points correspond to the Chandra observations in the range of faint fluxes, $f_X(0.5\text{–}2\,\mathrm{keV}) \approx 10^{-17}\text{–}10^{-15}$ erg s$^{-1}$ cm$^{-2}$, and to the XMM-Newton observations in the range $f_X(0.5\text{–}2\,\mathrm{keV}) \approx 10^{-15}\text{–}10^{-13}$ erg s$^{-1}$ cm$^{-2}$. It follows from the constructed curve of counts that the expected number of early-type galaxies to be detected during the eROSITA all-sky survey in the 0.5–2 keV band is ∼8400.

The emission from LMXBs in the 2–8 keV band dominates over the emission from the hot interstellar gas with a much softer spectrum. Therefore, to estimate the number of elliptical galaxies in the 2–8 keV band, we may neglect the contribution from the hot gas and assume that the entire emission from early-type galaxies is associated with compact sources—LMXBs. As was shown by Gilfanov (2004), the X-ray luminosity of LMXBs is linearly related to the near-infrared luminosity: $L_X[\mathrm{erg\,s^{-1}}] = 7.5 \times 10^{28} L_K[L_\odot]$. Using this relation and the observed $K$-band luminosity function of early-type galaxies (Kochanek et al. 2001), we can obtain the luminosity function of elliptical galaxies in the standard 2–8 keV X-ray band. Our calculations based on Eq. (1) by taking into account the survey sensitivity $S_0(2\text{–}8\,\mathrm{keV}) = 1.0 \times 10^{-13}$ erg s$^{-1}$ cm$^{-2}$ yield an estimate of ∼80 early-type galaxies to be detected in the 2–8 keV band during the all-sky survey by the eROSITA telescope. Note that this estimate, just as the estimate given at the end of the previous section, predicts the number of galaxies to be detected in the hard energy band independently of the information obtained in the 0.5–2.0 keV band. At the same time, the number of galaxies for which the 2–8 keV flux will be measured will be slightly larger.

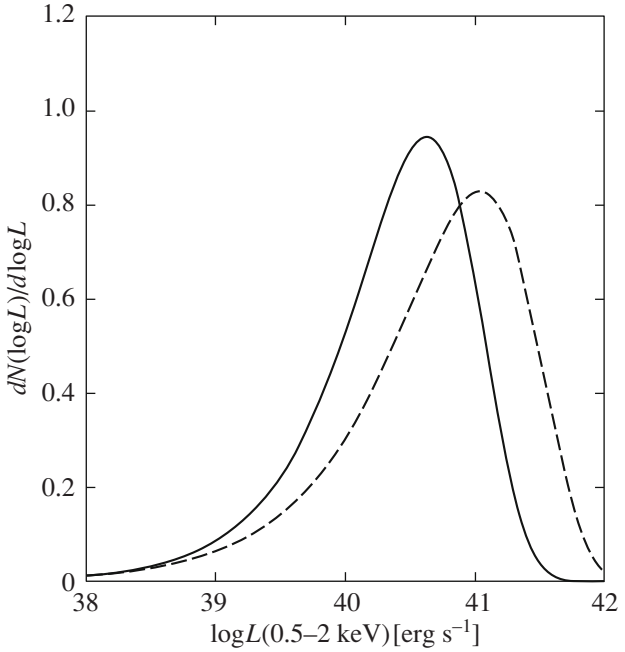


**Fig. 4.** Expected luminosity distributions of star-forming (solid line) and elliptical (dashed line) galaxies in the 0.5–2 keV in the eROSITA all-sky survey. The distributions were normalized to the same number of galaxies.

## THE DISTANCE AND LUMINOSITY DISTRIBUTIONS OF GALAXIES

Given the X-ray luminosity functions of star-forming and elliptical galaxies and the eROSITA sensitivity, we can determine the distance and luminosity distributions of normal galaxies to be detected in the survey:

$$N\,(d < D_L(z)) = \int_0^z dz' \frac{dV(z')}{dz'} \times \int_{\log L_{\min}(z')}^{\log L_{\max}} \phi(\log L, z') d\log L, \quad (4)$$

$$\frac{dN(L)}{d\log L} = \int_0^{z_{\max}(L)} \frac{dV(z)}{dz}\phi(\log L, z)dz, \quad (5)$$

where $\phi(\log L)$ is the luminosity function, $L_{\min}(z) = 4\pi D_L(z)^2 S_0$, $S_0$ is the survey sensitivity, $D_L(z)$ is the luminosity distance, and $z_{\max}$ is defined by the relation $L = S_0 4\pi D_L^2(z_{\max})$. In the integration based on Eqs. (4) and (5), we used the same observed luminosity functions in the 0.5–2 keV band as those used in counting the number of galaxies. The results of our calculations of $N(<D_L)$ and $dN(L)/d\log L$ are shown in Figs. 3 and 4. It follows from the figures that ~90% of the star-forming and elliptical galaxies to be detected in the survey are located within ~200 and ~400 Mpc, respectively, while the maxima of the differential distributions for both types of galaxies $dN(D_L)/dD_L$ lie at distances of ~70–90 Мпк. Figure 3 also shows the distance distributions for 10% of the brightest and 10% of the faintest galaxies. We see that the range of high fluxes in the $\log N - \log S$ distribution is attributable to nearby galaxies that are appreciably closer than the sample on average. Their distribution is at a maximum at a distance of ~30–40 Mpc. In contrast, the faintest galaxies are, on average, farther and are distributed almost uniformly at distances $\lesssim$300–500 Mpc. The maxima of the differential luminosity distribution $dN(L)/d\log L$ are reached at luminosities $\log L \sim 40.6$ and $\log L \sim 41.0$ for star-forming and elliptical galaxies, respectively. The luminosity distributions for 10% of the brightest and 10% of the faintest galaxies virtually coincide closely with that for the complete sample.

The typical luminosities of the galaxies in the survey can be correlated with the star formation rate (late-type galaxies) or the total stellar mass (early-type galaxies). The total X-ray luminosity of star-forming galaxies is proportional to the current star formation rate (Grimm et al. 2003; Ranalli et al. 2003; Shtykovkiy and Gilfanov 2005):

$$L_{0.5-2\,\mathrm{keV}}[\mathrm{erg\ s^{-1}}] \approx 2.2 \times 10^{39} SFR\,[M_\odot\ \mathrm{yr}^{-1}]. \quad (6)$$

Thus, the peak of the luminosity distribution for star-forming galaxies, $\log L\,[\mathrm{erg\ s^{-1}}] \sim 40.6$, corresponds to a star formation rate $SFR \sim 20 M_\odot\ \mathrm{yr}^{-1}$.

The main X-ray sources in elliptical galaxies are LMXBs and a hot interstellar gas. The dependence of the X-ray luminosity on the total stellar mass of the galaxy is different for these two types of sources. The luminosity attributable to LMXBs is directly proportional to the stellar mass of the galaxy (Gilfanov 2004):

$$L_{0.5-2\,\mathrm{keV}}[\mathrm{erg\ s^{-1}}] \sim 4 \times 10^{38} M_*[10^{10}\ M_\odot]. \quad (7)$$

The coefficient from Gilfanov (2004) that corresponds to early-type galaxies was corrected for the contribution from sources with a luminosity $\lesssim 10^{37}$ erg s$^{-1}$ and was recalculated to the 0.5–2 keV band by assuming a power-law spectrum with a photon index of 1.8 and absorption $N_{\mathrm{H}} = 3 \times 10^{20}$ cm$^{-2}$. Note that, in this case, the contribution from luminous soft sources with a luminosity $\log L_{\mathrm{X}} \sim 38.7$–$39.5$ is not taken into account quite accurately. Therefore, Eq. (7) slightly underestimates the total luminosity of the LMXBs in elliptical galaxies. The X-ray luminosity of the hot interstellar gas is related to the optical $B$-band

luminosity and the galaxy mass nonlinearly. This dependence has a large dispersion and, on average, can be described by the relation (O'Sullivan et al. 2001)

$$L_{0.5-2\,\mathrm{keV}}[\mathrm{erg\ s^{-1}}] \approx 5\times10^{23}L_B^{1.63}[L_\odot]. \quad (8)$$

To determine the mass-to-light ratio in the $B$-band, we will use the results of calculations from Bell and de Jong (2001): $\log(M/L_B) = -0.994 + 1.804(B-V)$. We will determine the mean color index for elliptical galaxies from optical observations of early-type galaxies (Michard and Prugniel 2004), $\langle B-V\rangle \approx 0.93$. Expressing the $B$-band luminosity in terms of the stellar mass using (7), $M_*/L_B \approx 4.8$, and substituting it into (8) yields the dependence of the soft X-ray luminosity for the hot interstellar gas on the stellar mass of the galaxy:

$$L_{0.5-2\,\mathrm{keV}}\,[\mathrm{erg\ s^{-1}}] \approx 5.8\times10^{38}M_*^{1.63}[10^{10}\,M_\odot]. \quad (9)$$

Comparing (7) and (9), we find that the soft X-ray emission from the hot interstellar gas in luminous massive elliptical galaxies, $M_* \gtrsim 10^{10}M_\odot$ ($L_{0.5-2\,\mathrm{keV}} \gtrsim 10^{39}$ erg s$^{-1}$), dominates over the emission from compact sources—LMXBs. The peak of the luminosity distribution for early-type galaxies in the eROSITA survey located at $L_\mathrm{X} \sim 10^{41}$ erg s$^{-1}$ (Fig. 4) corresponds to massive elliptical galaxies with $M \sim 2\times10^{11}M_\odot$ emitting in the soft X-ray band mainly through a hot interstellar gas with a soft spectrum. In particular, this is responsible for the significant contrast in the number of early-type galaxies to be detected in the soft and hard energy bands.

Given the luminosity distribution of the observed galaxies, we can assess the potentialities of the survey in measuring the X-ray luminosity function of normal galaxies, in particular, at low luminosities. The currently existing soft X-ray luminosity functions of galaxies were constructed for luminosities higher than $10^{39}$ erg s$^{-1}$ and, as has already been noted above, were constructed from samples containing several tens of galaxies. The shape of the luminosity function at lower luminosities is unknown. Therefore, we will make an estimate for two shapes of the luminosity function: (1) by extrapolating the observed power law to the range $L_{0.5-2\,\mathrm{keV}} < 10^{39}$ erg s$^{-1}$ and (2) by assuming that $dN(L)/d\log L = \mathrm{const}$ for $L_{0.5-2\,\mathrm{keV}} < 10^{39}$ erg s$^{-1}$. For these luminosity functions, the number of galaxies to be detected in the luminosity range $38 < \log L_{0.5-2\,\mathrm{keV}} < 38.5$ is ~20–60 and ~20–70 for late- and early-type galaxies, respectively. Theoretically, this will allow the luminosity function to be determined with an accuracy of ~10–20%.

## CORRELATION WITH INFRARED SKY SURVEYS

Let us compare the sensitivity of the eROSITA all-sky survey with the near-infrared (Two Micron All Sky Survey—2MASS) and far-infrared (Infrared Astronomical Satellite—IRAS) surveys. Recall that the near- and far-infrared emissions characterize the stellar mass and the current star formation rate in galaxies. Therefore, comparison with these catalogs will be an integral part of the analysis and interpretation of the eROSITA data.

The IRAS catalog of point sources is statistically complete to fluxes of 0.6 and 1.0 Jy at wavelengths of 60 and 100 $\mu$m, respectively. Using the relation between the far-infrared and soft X-ray luminosities for star-forming galaxies, $L_\mathrm{X} \approx 2.1\times10^{-4}L_\mathrm{FIR}$ (Ranalli et al. 2003), let us transform this value to the soft X-ray flux, $S(0.5–2\,\mathrm{keV}) \approx (5–9)\times10^{-15}$ erg s$^{-1}$ cm$^{-2}$. This value is close to our sensitivity threshold (~$10^{-14}$ erg s$^{-1}$ cm$^{-2}$); therefore, both catalogs will contain approximately the same sample of star-forming galaxies (since the sensitivity of the IRAS catalog is slightly better, its sample will be slightly larger). Thus, from the standpoint of investigating star-forming galaxies, the eROSITA all-sky survey is equivalent to the IRAS one.

2MASS has a sensitivity at 2.2 $\mu$m ($K$ band) $m_K < 13.5$. Because of the nonlinear relation between the gas X-ray luminosity and the galaxy mass, the X-ray flux from an early-type galaxy with $m_K = 13.5$ depends on the distance—more distant galaxies will have higher masses and, accordingly, larger contributions to the hot-gas luminosity. For nearby galaxies, $D \lesssim 20–30$ Mpc, $S(0.5–2\,\mathrm{keV}) \approx (2-3)\times10^{-16}$ erg s$^{-1}$ cm$^{-2}$; the flux increases with distance but it does not exceed the sensitivity threshold even for the most distant galaxies in our survey: $S(0.5–2\,\mathrm{keV}) \approx (2-3)\times10^{-15}$ erg s$^{-1}$ cm$^{-2}$ at $D = 500$ Mpc. Thus, one would expect that all of the early-type galaxies to be detected in the eROSITA all-sky survey enter into the 2MASS catalog. However, in contrast to the situation with star-forming galaxies, 2MASS is a much deeper survey.

Thus, a large, statistically homogeneous sample of normal galaxies with measured X-ray, near-infrared, and far-infrared fluxes will be formed as a result of the eROSITA all-sky survey.

## ULTRALUMINOUS X-RAY SOURCES IN THE eROSITA SURVEY

According to the universally accepted (but not quite clear) definition, the sources with luminosities exceeding ~$10^{39}$ erg s$^{-1}$, the Eddington luminosity limit for a black hole with a mass of ~$10M_\odot$, are

called ultraluminous ones (ULXs). Based on an analysis of the luminosity function for compact sources in nearby star-forming galaxies, Grimm et al. (2003) concluded that the low end of the luminosity range, $\log L_X \lesssim 39.5$–$39.7$, is probably an extension of the population of accreting stellar-mass black holes in high-mass X-ray binaries. The number of more luminous sources, $\log L_X \gtrsim 40$, in the sample of Grimm et al. (2003) was insufficient for a reliable determination of their luminosity function. The relatively few studies of the properties of individual sources could not unambiguously answer the question about their nature either. Let us assess the potentialities of the all-sky survey in investigating these sources.

In galaxies with a high star formation rate that contain many ULXs and that are more than several tens of Mpc away, the angular resolution of the eROSITA telescope will be too low to resolve luminous sources into individual objects. At distances of ~35 Mpc, an angular resolution of ~30″ corresponds to a linear size of ~5 kpc, i.e., on average, ~1/3–1/2 of the linear size of the Galaxy. In this case, two sources located, for example, at the center and on the periphery of a galaxy can be spatially resolved by eROSITA. Therefore, for a rough estimate, we will take into account only the galaxies located at distances $d < d_{max} = 35$ Mpc. As the luminosity threshold, we will choose $10^{40}$ erg s$^{-1}$ in the 0.5–8 keV band, which corresponds to a luminosity $\approx 3 \times 10^{39}$ erg s$^{-1}$ in the 0.5–2 keV band, by assuming a power-law spectrum with $\Gamma = 1.74$ and $N_H = 2.2 \times 10^{21}$ cm$^{-2}$ (Swartz et al. 2004). The flux for a source with such a luminosity located at a distance of 35 Mpc is $\sim 2 \times 10^{-14}$ erg s$^{-1}$ cm$^{-2}$, which is twice the sensitivity threshold of the survey. Thus, the sensitivity of the survey will be sufficient to potentially detect all sources with a soft X-ray luminosity $L_X > L_{lim} = 3 \times 10^{39}$ erg s$^{-1}$ located within 35 Mpc. The total number of such sources is

$$N_{ULX} = V \int \frac{dN_{gal}}{dSFR} N_X(L_{lim}, SFR) dSFR, \quad (10)$$

where $V$ is the volume of the sphere with a radius of 35 Mpc, $N_X(L_{lim}, SFR) = 2 \times SFR \times (L_{lim}^{-0.6} - L_{max}^{-0.6})/(10^{38})^{-0.6}$ is the number of compact sources with a luminosity $L_X > L_{lim}$ (0.5–8 keV) in a galaxy with a star-formation rate $SFR\ M_\odot$ yr$^{-1}$, $L_{max} = 2.1 \times 10^{40}$ erg s$^{-1}$ in the 0.5–8 keV band (Grimm et al. 2003; Shtykovkiy and Gilfanov 2005). Note that the number of luminous sources $N_X(L_{lim}, SFR)$ depends strongly on the exact value of $L_{max}$ and the behavior of the luminosity function near it, which are unknown due to the limited number of the most luminous sources known to date. We will determine the distribution of galaxies in star formation rate, $dN_{gal}/dSFR$, from the radio luminosity function of galaxies at 1.4 GHz specified by Eq. (2) and from the relation between the radio luminosity of star-forming galaxies and the star formation rate: $SFR[M_\odot\ \mathrm{yr}^{-1}] \approx 5.5 \times 10^{-29} L_{1.4\,GHz}[\mathrm{erg\ s^{-1}\ Hz^{-1}}]$ (Bell 2003).

Our calculation based on Eq. (10) gives $N_{ULX} \approx 85$. We emphasize once again that this number depends on the behavior of the luminosity function for ULXs in the range of high luminosities, which is not known exactly. The fraction of the ULXs located in galaxies with an expected number of sources $N(L_X > 3 \times 10^{39} \mathrm{erg\ s^{-1}}) < 1$ is ~80%. Thus, most of them will dominate in the emission of their host galaxies and will be spatially resolvable. Although an adequate luminosity function of ULXs in galaxies cannot be constructed, the survey data will allow us to impose constraints on the luminosity distribution of the most luminous sources and, probably, to determine their maximum luminosity.

## MODELING THE IMAGES OF THE GALAXIES NGC 4038/4039 AND M51

To illustrate the difficulties that will arise in investigating even the brightest compact sources in galaxies, we modeled the images of two nearby star-forming galaxies. The Antennae galaxies (NGC 4038/4039) are a pair of interacting galaxies with a high star formation rate, $\sim 20 M_\odot$ yr$^{-1}$, located at a distance of 19.3 Mpc. A large population of ultraluminous X-ray sources, 18 sources with luminosities higher than $10^{39}$ erg s$^{-1}$ (Zezas et al. 2002), is located in them. M51 is a star-forming galaxy with a star formation rate of $\sim 12 M_\odot$ yr$^{-1}$ locate at a distance of 7.5 Mpc.

When modeling the images, we used the Chandra observations of these galaxies. To transform these images into the eROSITA energy band and response matrix, we assumed a power-law spectrum with a photon index of 1.7 and absorption $N_H = 3 \times 10^{20}$ cm$^{-2}$. To take into account the difference in spatial resolution, we used the convolution with a Gaussian distribution whose width corresponded to the eROSITA angular resolution $\sigma = 12\farcs3$. The images were rebinned into larger pixels with sizes $7\farcs8 \times 7\farcs8$ (M51) and $3\farcs9 \times 3\farcs9$ (Antennae) and Poisson noise was added.

The images obtained are shown in Fig. 5. We see that the Antennae galaxies are unsuitable for investigating individual compact sources due to the large number of ultraluminous sources. In the case of M51,

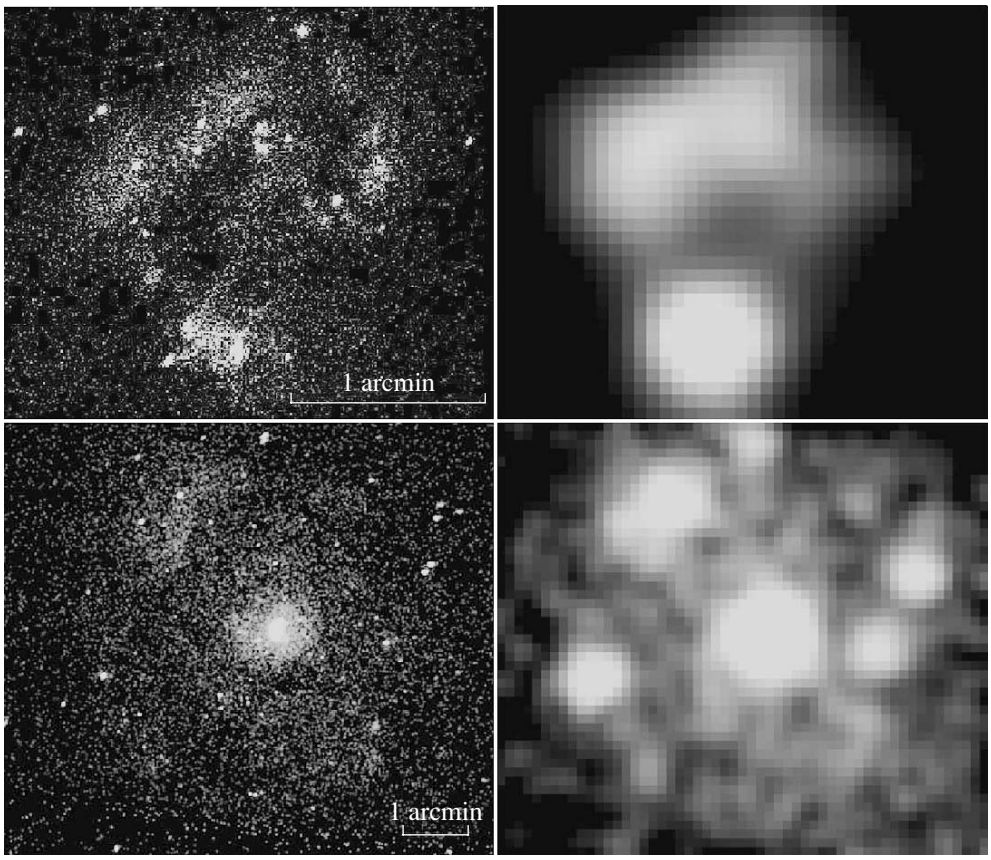


**Fig. 5.** Images of the galaxies NGC 4038/4039 (top) and M51 (bottom) in the 0.5–2 keV band. The original Chandra images are shown on the left; the modeled images of these galaxies to be obtained in the 4-year all-sky survey are shown on the right. The modeled images were convolved with a Gaussian $(1\sigma) \approx 10''$ in width to smooth out the statistical Poissonian noise.

with a factor of ∼2 lower star formation rate and located a factor of ∼2–3 closer, the contribution from the most luminous sources can be resolved. Note that the example of the Antennae galaxies illustrates the most unfavorable situation—the fraction of the ultraluminous sources within 35 Mpc located in galaxies with comparable and higher star formation rates will not exceed ∼20%.

## CONCLUSIONS

We analyzed the main statistical properties of normal galaxies to be detected in the all-sky survey by the eROSITA X-ray telescope of the Spectrum-X-Gamma observatory.

(1) The expected numbers of normal late-type (∼star-forming) and early-type (∼elliptical) galaxies to be detected in the 0.5–2 keV (2–8 keV) band are ∼7200–10 000 (∼300–400) and ∼8400 (∼80), respectively. All or almost all of the galaxies enter into the existing far-infrared (IRAS) and near-infrared (2MASS) sky surveys. The sample of star-forming galaxies will be approximately equivalent to that in the IRAS catalog of infrared sources. Thus, a large homogeneous sample of normal galaxies with measured X-ray, near-infrared, and far-infrared fluxes will be formed as a result of the eROSITA all-sky survey.

(2) Approximately 90% of the galaxies in the survey are located within $\lesssim$200–400 Mpc, with the most probable distance (the maximum of the differential distribution) for both types of galaxies being ∼70–90 Mpc. Ten percent of the brightest galaxies are located closer, at distances ∼30–40 Mpc, while 10% of the faintest galaxies are distributed more uniformly up to distances $\lesssim$300–500 Mpc.

(3) The maxima of the luminosity distributions $dN/d\log L$ are reached at luminosities $\log L \sim 40.6$ and $\log L \sim 41$ for star-forming and elliptical galaxies, respectively. Thus, star-forming galaxies with a relatively high star formation rate, $SFR \sim 20 M_\odot\ \mathrm{yr}^{-1}$, and massive elliptical galaxies with a stellar mass $\log M_* \sim 11.3$ will be most probable in the survey. The soft X-ray emission from the latter is attributable mainly to a hot interstellar gas.

(4) The expected number of ultraluminous X-ray sources ($L_X > 10^{40}$ erg s$^{-1}$ in the 0.5–8 keV band) in galaxies within 35 Mpc is ∼85. In this case, ∼80%

of them will be in galaxies with an expected number of ULXs <1. Thus, the all-sky survey will allow constraints to be imposed on the bright end of the luminosity function for ULXs and, possibly, their luminosity limit to be estimated.

## ACKNOWLEDGMENTS

We wish to thank P. Predehl for a detailed discussion of the eROSITA configuration and the characteristics of various instrumental background components and for providing a preliminary response matrix of the telescope. We are grateful to the referee A. Vikhlinin for constructive remarks. I. Prokopenko thanks EARA (European Association for Research in Astronomy; MEST-CT-2004-504604) for support by Marie Curie's grant and the Max-Planck-Institut für Astrophysik, in which much of this work was performed, for hospitality. I. Prokopenko was supported by grant no. NSh-5579.2008.2 from the President of Russia and the Russian Academy of Sciences ("Origin and Evolution of Stars and Galaxies" Program).

## REFERENCES

1. E. F. Bell, Astrophys. J. **586**, 794 (2003).
2. E. F. Bell and R. S. de Jong, Astrophys. J. **550**, 212 (2001).
3. A. E. Georgakakis, V. Chavushyan, M. Plionis, et al., Mon. Not. R. Astron. Soc. **367**, 1017 (2006a).
4. A. E. Georgakakis, I. Georgantopoulos, A. Akylas, et al., Astrophys. J. **641**, 101 (2006b).
5. I. Georgantopoulos and P. Tzanavaris, arXiv:0801.4386 (2008).
6. M. Gilfanov, Mon. Not. R. Astron. Soc. **349**, 146 (2004).
7. H.-J. Grimm, M. Gilfanov, and R. Sunyaev, Mon. Not. R. Astron. Soc. **339**, 793 (2003).
8. R. C. Hickox and M. Markevitch, Astrophys. J. **645**, 95 (2006).
9. C. S. Kochanek, M. A. Pahre, E. E. Falco, et al., Astrophys. J. **560**, 556 (2001).
10. J. Machalski and W. Godlowski, Astron. Astrophys. **360**, 463 (2000).
11. R. Michard and P. Prugniel, Astron. Astrophys. **423**, 833 (2004).
12. A. Moretti, S. Campana, D. Lazzati, et al., Astrophys. J. **588**, 696 (2003).
13. E. O'Sullivan, D. A. Forbes, and T. J. Ponman, Mon. Not. R. Astron. Soc. **328**, 461 (2001).
14. A. Ptak, B. Mobasher, A. Hornschemeier, et al., Astrophys. J. **667**, 826 (2007).
15. P. Ranalli, A. Comastri, and G. Setti, Astron. Astrophys. **399**, 39 (2003).
16. P. Ranalli, A. Comastri, and G. Setti, Astron. Astrophys. **440**, 23 (2005).
17. P. Shtykovkiy and M. Gilfanov, Astron. Astrophys. **431**, 597 (2005).
18. R. C. Smith, N. S. Brickhouse, D. A. Liedahl, et al., Astrophys. J. **556**, 91 (2001).
19. D. N. Spergel, R. Bean, O. Dor, et al., Astrophys. J. **170**, 377 (2007).
20. D. A. Swartz, K. K. Ghosh, A. F. Tennant, et al., Astrophys. J. **154**, 519 (2004).
21. A. Zezas, G. Fabbiano, A. H. Rots, et al., Astrophys. J. Suppl. Ser. **142**, 239 (2002).

*Translated by V. Astakhov*